

NUMERICAL MODELING ON PROSPECTIVE BUFFER LAYERS FOR TUNGSTEN DI-SULFIDE (WS₂) SOLAR CELLS BY SCAPS-1D

K. SOBAYEL^a, K. S. RAHMAN^{a,b}, M. R. KARIM^c, M. O. AIJAZ^c, M. A. DAR^c,
M. A. SHAR^c, H. MISRAN^b, N. AMIN^{b*}

^a*Department of Electrical, Electronic and Systems Engineering, Faculty of Engineering and Built Environment, The National University of Malaysia, 43600 Bangi, Selangor, Malaysia*

^b*Institute of Sustainable Energy, Universiti Tenaga Nasional (@The National Energy University), Jalan IKRAM-UNITEN, 43000 Kajang, Selangor, Malaysia*

^c*Center of Excellence for Research in Engineering Materials (CEREM), Deanship of Scientific Research, King Saud University, Riyadh 11421, Kingdom of Saudi Arabia*

In this study, tungsten di-sulphide (WS₂), one of the key transition-metal dichalcogenide (TMDC) materials, is used as solar cell absorber material with a suitable solar cell configuration and analyzed by SCAPS-1D. Other main focuses include optimum absorber layer thickness, suitable material for buffer layer instead of CdS and effect of operating temperature on solar cell performance. An efficiency of 19.48% (with V_{oc} of 0.90 V, J_{sc} of 24.94 mA/cm² and fill factor of 0.86) has been found for the cell with CdS based buffer layer. High efficiency WS₂ solar cells have the optimized absorber thickness in the range of 2 μm to 3 μm. Moreover, the desired thickness of the buffer layer is observed in between 40–60 nm. Among different types (ZnO, ZnSe, ZnS, CdS and In₂S₃) of buffer layers, ZnO based WS₂ solar cell shows the potential to reach out the highest efficiency of 25.71%. However, cell with ZnO buffer layer shows a temperature gradient of -0.24%/K. All these simulation results provide significant hints that may lead to higher efficiency of WS₂ solar cells with beneficial experimental studies in practical implementation.

(Received December 1, 2017; Accepted June 1, 2018)

Keywords: TMDC; WS₂; ZnO; SCAPS; buffer layer; temperature gradient.

1. Introduction

Energy is indispensable for financial development in any country and a key element to alleviate poverty. The worldwide energy framework is in the phase of convulsion these days. The venvy for green energy to fulfill the ever-growing world's energy need has prompted the researcher's community to focus their research on renewable energy arena. Among the candidates of the solar cells, thin film solar cells especially inexpensive, earth abundant and nontoxic materials like tungsten di-sulfide (WS₂) has attracted an increasing interest. WS₂ is a layer type semiconductor that exhibits similar structured materials like graphite or mica [1, 2]. It is well known as transition-metal dichalcogenides (TMDC) like MoS₂, MoS(Se)₂, WS₂ and WS(Se)₂, which are all potential semiconductors. TMDCs particularly MoS₂ and WS₂ raised special concern to photovoltaic community as absorber layer material in thin-film solar cells [3, 4]. This is due to their suitable bandgaps (1-2 eV) and the very high absorption coefficients which is over 10⁵ cm⁻¹ [4]. Though single crystals of this material have been extensively studied for optical equipment; only a few studies have been carried out on the photovoltaic properties of thin film. About 30 years ago, TMDCs were studied as semiconductors for solar cells with a liquid electrode [3, 5]. To fabricate thin-film solar cells, polycrystalline WS₂ films were used for the last one decade [6, 7].

*Corresponding author: nowshad@uniten.edu.my

However, researchers are yet to fabricate high efficiency WS₂ solar cells. Among the researchers in WS₂ community, only Jäger–Waldau et al. reported solar-cell device data of planar cells with an efficiency below 1% (<0.31%) [6].

Numerical simulation is a primary step to determine the optimize structure of a solar cells. Presently, there is a lack of numerical simulation report about WS₂ solar cells. Therefore, with a view to develop high efficiency, earth abundant WS₂ solar cell; a numerical simulation based on SCAPS-1D is performed to investigate the desired thickness of absorber and buffer layer and also to find a suitable material for buffer layer. Moreover, ambient operational temperature has been taken into consideration in this study.

2. Numerical Modeling and Material Parameters

A Solar Cell Capacitance Simulator (SCAPS) is one-dimensional computer simulation software for simulating alternating current and direct current electrical attributes of thin film heterojunction solar cells. Although it was fostered to analyze mainly CdTe and CIGS based solar cells but presently SCAPS is widely used to investigate and replicate the characteristics of all types of solar cells with different buffer layers. SCAPS has a unique way to show simulation outputs. It has unique properties such as simulation of current voltage characteristics both in dark and under illumination. In this paper, Solar Cell Capacitance Simulator (SCAPS-1D) is used to analyses the WS₂ based solar cells. It was developed in ELIS, University of Gent and later made freely available to the photovoltaic research community [8-10]. SCAPS is highly popular among researchers of PV community for its good agreements between the experimental results and the SCAPS simulation results and that motivates to use this simulation tool in research work [13-15].

SCAPS can solve the basic semiconductor equations namely the Poisson's equation for electrons and holes is (Eqs. (1) - (3)) [11, 12]

$$d^2\psi(x)/dx^2 = e/\epsilon_0\epsilon_r (p(x) - n(x) + N_D - N_A + \rho_p - \rho_n) \quad (1)$$

Where ψ = electrostatic potential, e = electrical charge,
 ϵ_r = relative permittivity ϵ_0 = vacuum permittivity,
 N_D = charged impurities of donor N_A = acceptor charged impurities,
 ρ_p = holes distribution ρ_n = distribution of electrons

The equations of continuity for electrons and holes are:

$$dJ_n/dx = G - R \quad (2)$$

$$dJ_p/dx = G - R \quad (3)$$

For semiconducting materials, carrier transport occurs by drift and diffusion and can be expressed by following equations:

$$J_n = D_n dn/dx + \mu_n n d\phi/dx \quad (4)$$

$$J_p = D_p dp/dx + \mu_p p d\phi/dx \quad (5)$$

Here, R is the rate of recombination, J_p and J_n are hole and electron current densities and G is the generation rate. This simulation software calculates solution of the basic semiconductor equations in 1-D state and in steady conditions.

A typical WS₂ solar cell structure comprises a Molybdenum (Mo) coated glass substrate where a p-type absorber layer (WS₂) is deposited on top of it. n-CdS (CdS, ZnO, ZnS, ZnSe, In₂S₃) or any suitable n-type material is used as buffer layer and window layer is made of n-ZnO: Al. The cell is illustrated schematically in Fig. 1. It is a matter of fact that there is hardly any work done on WS₂ solar cell by using simulation. However, SCAPS is used to depict high efficiency WS₂ solar cells with desired absorber thickness and suitable buffer layer as well. Five buffer layers, n-type

ZnO, ZnSe, ZnS, CdS and In_2S_3 are emphasized in this simulation. By assimilating different material parameters into SCAPS; V_{oc} , J_{sc} , efficiency and FF of WS_2 solar cell with different buffer layers and effect of operating temperature on those are observed. Simulation parameters for a standard WS_2 solar cell are summarized in Table 1.

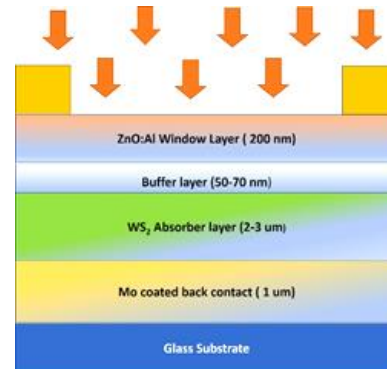


Fig. 1. Schematic diagram of WS_2 solar cell

Table 1. The parameters for the WS_2 solar cell at 300K

Parameter	WS_2	CdS	ZnS	In_2S_3	ZnO	ZnSe	ZnO: Al
Thickness (nm)	2000	50	60	50	60	60	200
Permittivity, ϵ_r	13.6	9	10	13.5	9	10	9
Electron Affinity (eV)	4.05	4.2	3.9	4.7	4.45	2.9	4.6
Bandgap, E_g (eV)	1.29	2.4	3.5	2.8	3.3	2.7	3.3
Density of States, N_c ($1/\text{cm}^3$)	$2.20\text{E}+18$	$2.20\text{E}+18$	$1.50\text{E}+18$	$2.20\text{E}+18$	$2.20\text{E}+18$	$1.50\text{E}+18$	$2.20\text{E}+18$
Density of States, N_v ($1/\text{cm}^3$)	$1.80\text{E}+19$	$1.80\text{E}+19$	$1.80\text{E}+19$	$1.80\text{E}+19$	$1.80\text{E}+19$	$1.80\text{E}+18$	$1.80\text{E}+19$
Electron Mobility ($\text{cm}^2/\text{V s}$)	100	100	165	400	100	50	100
Hole Mobility ($\text{cm}^2/\text{V s}$)	100	25	5	210	25	20	25
Donor Concentration ($1/\text{cm}^3$)	0	$1.00\text{E}+17$	$1.00\text{E}+16$	$1.00\text{E}+17$	$1.00\text{E}+18$	$1.00\text{E}+17$	$1.00\text{E}+18$
Acceptor Concentration ($1/\text{cm}^3$)	$1.00\text{E}+18$	0	0	10	0	0	0
Gaussian Defect ($1/\text{cm}^3$)	$1.00\text{E}+18$	$1.00\text{E}+17$	$1.00\text{E}+17$	$1.00\text{E}+18$	$1.00\text{E}+18$	$1.00\text{E}+17$	$1.00\text{E}+18$

3. Result and Discussions

3.1 Optimization of WS_2 Absorber Thickness

To validate the simulation, a standard CIGS absorber with CdS buffer layer based structure has been considered in terms of WS_2 absorber layer. The standard thickness of the Cu (In, Ga) Se_2 layer in CIGS solar cells is about 3000 nm. If this thickness is reduced, with or without minor loss in the performance, the deposition time of CIGS layer can also be reduced [22]. This facilitates the reduction of materials usage in large scale deposition and thereby overall production costs are reduced [17]. Abatement of usage of materials and cost are important parameters for PV industry. However, it is not always preferred to reduce thickness of absorber

layer as it may leads to some unwanted problems [16]. Keeping it into consideration, the WS_2 absorber thickness has been varied from 1000-5000 nm to ascertain the desired thickness based on CIGS structure with CdS as buffer layer. While varying the absorber thickness with SCAPS-1D, the properties of the different layers are kept constant. The bandgap of the absorber is also kept constant to 1.29 eV [4]. It is revealed that the efficiency escalates with the increase of thickness of the WS_2 absorber layer, but with a much slower rate over 2000 nm. Simulation results suggest that optimum thickness for WS_2 absorber layer would be around 2000-3000 nm. It is found that at 1000 nm and 5000 nm absorber thickness, the recorded efficiency is 16.74% and 21.95%, respectively.

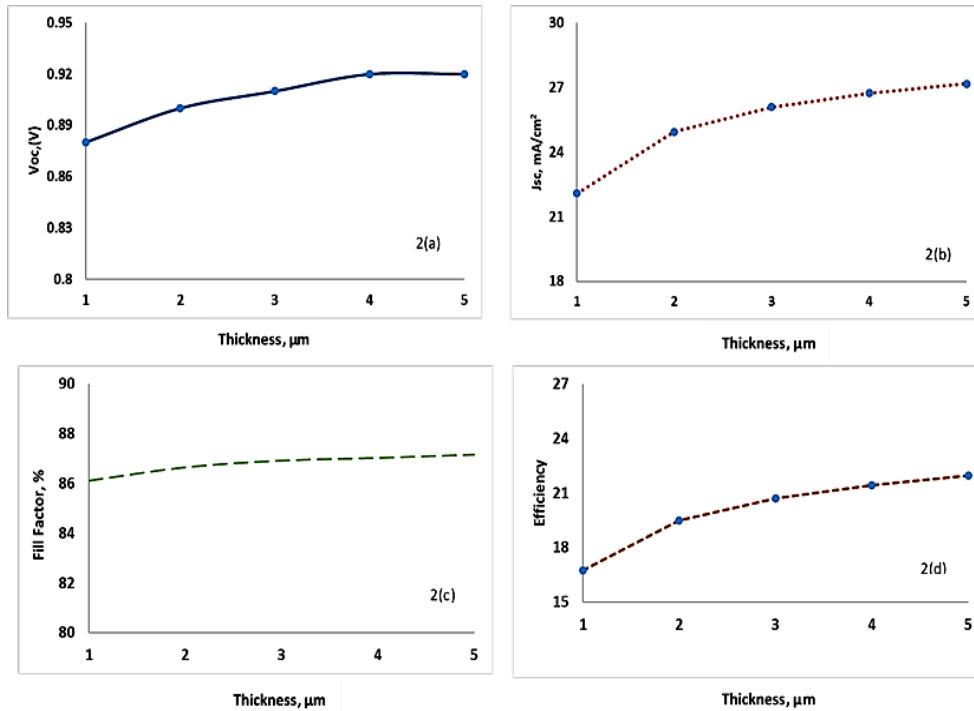


Fig. 2. (a) Change of V_{oc} (V) with variable thickness of WS_2 absorber layer. (b) Change of J_{sc} (mA/cm^2) with different absorber thickness. (c) Measurement of Fill Factor of different absorber thickness. (d) Cell performance (efficiency, %) with variable thickness of WS_2 absorber layer

Photovoltaic parameters (J_{sc} , V_{oc} , FF and efficiency) of WS_2 solar cells with different absorber thicknesses are shown in Fig. 2. All the values are escalating with the increased thickness of the absorber layer. The reason is that the thicker absorber layer is more capable of retaining higher number of photons than thinner layer. That in turn generates more electron-hole pairs [18]. It is noted that J_{sc} is almost linear from 3000 nm -5000 nm thickness. In other words, J_{sc} decreases almost linearly with the decrease of thickness but with little higher gradient once thickness is reduced to below 2000 nm. It might be due to incomplete absorption of incident photons and recombination process at back contact of the cell. When absorber layer thickness is taken off, the back contact remains extremely close to the depletion area. Thus, back contact material can easily capture electrons for the recombination process. In this way, lesser number of electrons can add to the quantum efficiency of the solar cell and the J_{sc} becomes low.

It is revealed that efficiency decreases at lower rate (0.082%) if thickness is reduced from 5000 nm to 2000 nm. Again, it was found that with every 1000 nm reduction of absorber thickness from 2000 nm caused decrease in efficiency by 0.274%. It affirms that the thickness of 2000 nm is enough to absorb most of the incident photons. Therefore, for large scale production or industrial purpose where processing times and material usage play a big role; fabricating WS_2 solar cells with thick absorber layer will not be viable and cost effective. So, later here in numerical simulation, WS_2 layer thickness is adopted at 2000 nm.

3.2 Effect of CdS Buffer Layer Thickness

Earlier, it has been identified that the optimum thickness of CdS buffer layer is within the range of 50 nm - 60 nm [19]. The thickness of buffer layer (CdS) was diverged from 10 nm to 90 nm in this simulation. The effect of the varying thickness of CdS buffer layer is shown in Fig 3. It is found that there is no significant effect on V_{oc} , J_{sc} or even in efficiency with the change of buffer layer thickness. A thicker buffer layer absorbs energy carried by photon resulting in higher number of photon loss [20]. A lower number of photons at the absorber layer would decrease the quantum efficiency of the solar cell as shown in Fig. 4. Again, it appeared that the Fill factor and efficiency of thin buffer layer (< 50 nm) are comparatively low. It may be because of leakage current that produces from too thin buffer layer. On the other hand, too thick buffer layer may lead to low carrier separation rate [18]. Considering above, the optimized and preferred buffer layer thickness would be from 50 nm to 70 nm. In this paper, thickness of buffer layer is considered to be 50 nm, which is found as optimum from the simulation results.

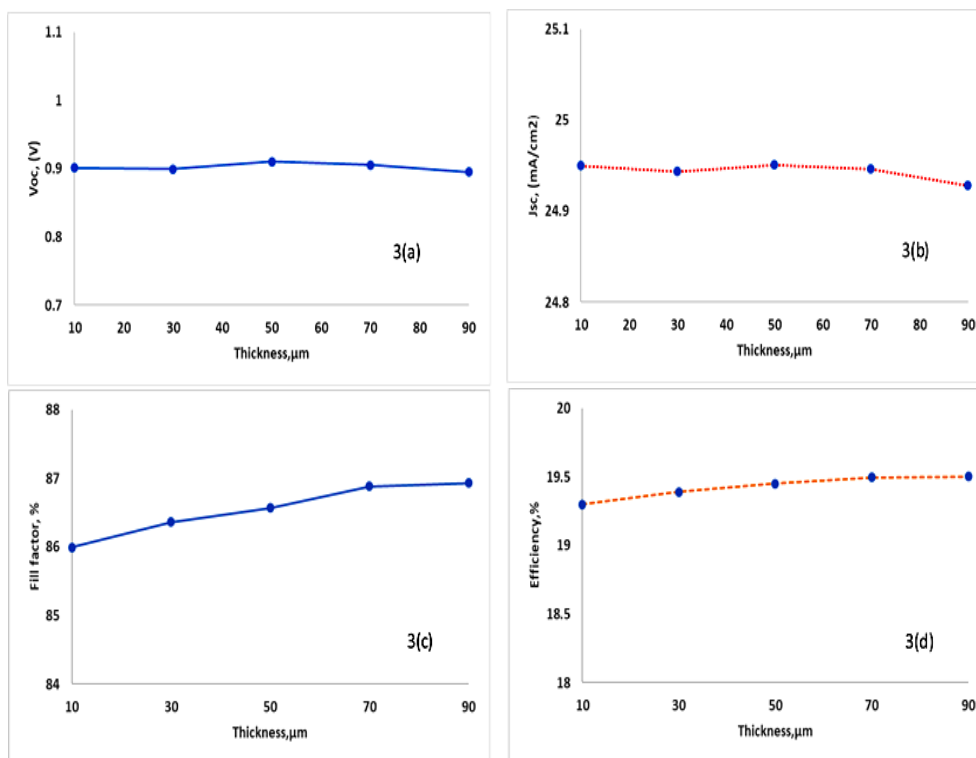


Fig. 3. (a) Change of V_{oc} (V) with variable thickness of CdS buffer layer. (b) Effect on J_{sc} (mA/cm²) with different buffer layer thickness. (c) Measurement of Fill Factor with different thickness of CdS buffer. (d) Cell performance (efficiency, %) with variable thickness of CdS buffer layer

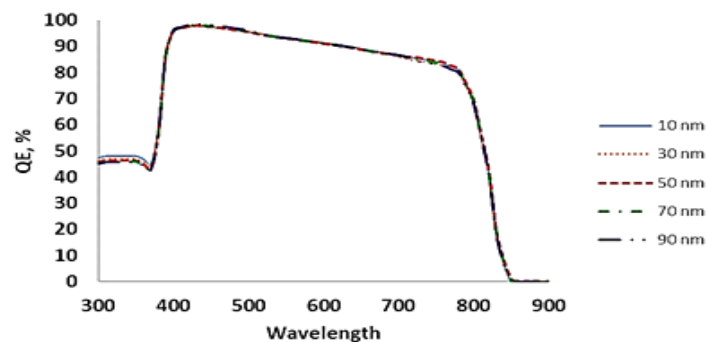


Fig 4: Spectral response of solar cells with variable thickness of CdS buffer layer

3.3 Effect of Different Buffer Layers on Cell Performance

CdS is toxic and cadmium compounds are classified as carcinogenic, which is hazardous to human health. Therefore, other potential buffer layers such as ZnS, In_2S_3 , ZnSe and ZnO have also been investigated. Fig. 5 shows the simulated J-V characteristics with the AM1.5 illumination conditions (100 mW/cm^2), for different buffer layers. Fig. 6 shows the comparative study (V_{oc} , J_{sc} , FF and η) of different buffer layers. Fig. 7 shows QE (%) of different buffer layers on light spectrum. It is noted that buffer layer thickness is considered as 50 nm, which is found optimum for CdS as buffer layer in WS_2 solar cell. From the simulation result, it is also found that ZnO and ZnSe based buffer layers give the highest conversion efficiency of 25.71% and 25.63%, respectively. Apart from these two, ZnS and In_2S_3 based buffer layers have achieved efficiencies of 10.03% and 22.4%, respectively. Hence, ZnO and ZnSe are highly promising candidate as buffer layer to replace CdS buffer layer in WS_2 based solar cell.

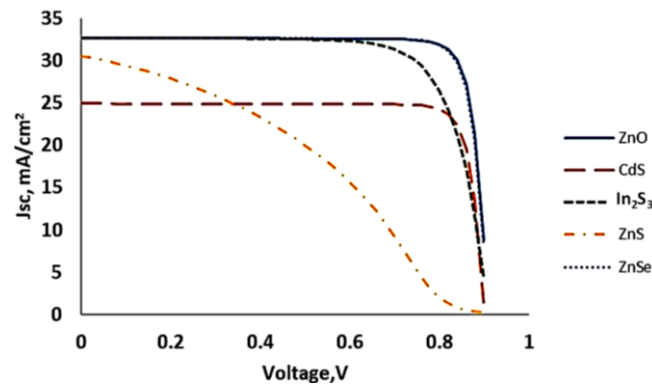


Fig. 5. J-V characteristics of cells with different buffer layer

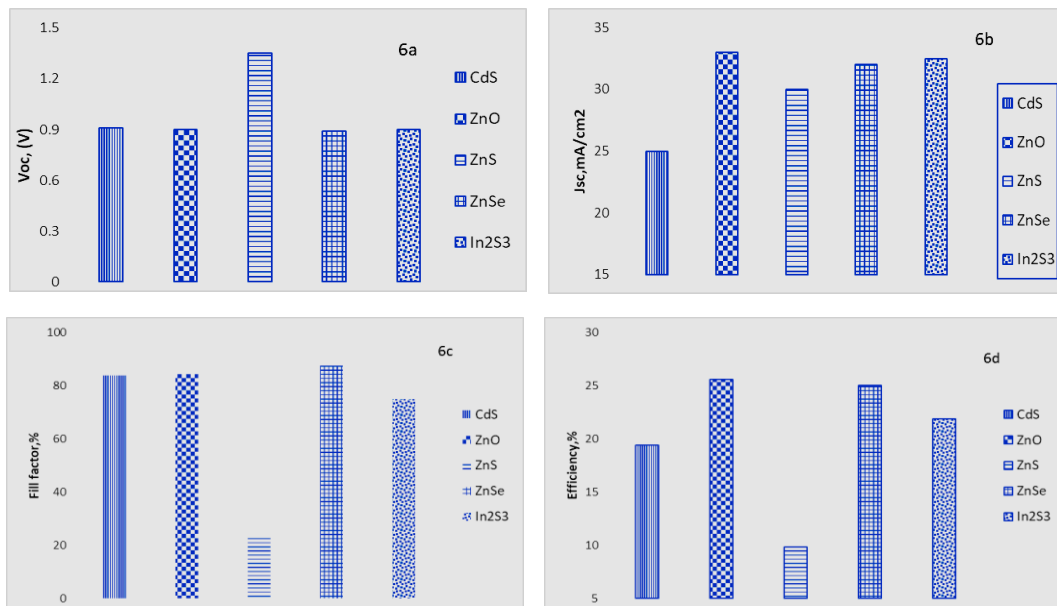


Fig. 6. (a) Change of V_{oc} (V) with variable buffer layers. (b) Change of J_{sc} (mA/cm^2) with different buffer layers. (c) Measurement of Fill Factor of different buffer layers. (d) Cell performance (efficiency, %) with different buffer layers

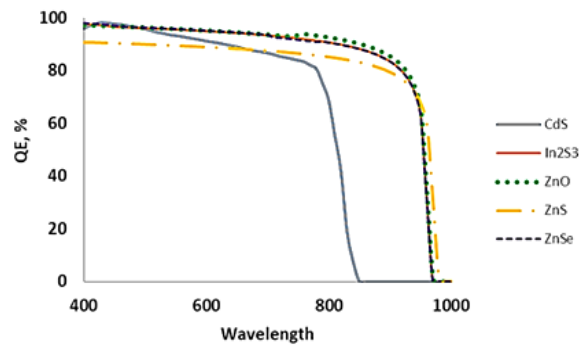


Fig. 7. Spectral response of solar cells with different buffer layers

3.4 Effects of Operating Temperature on WS₂ Solar Cells with Various Buffer Layer

Operating temperature has a significant role in the performance of the solar cells. Solar panels are generally installed in the open environment. Thus, sunlight falls on it directly and causes increase in temperature. Practically, solar panels are heated by sunshine at higher temperature than 300 K (up to 370K) in tropical countries. The effect of working temperature on the performance of WS₂ solar cell has been investigated by changing operating temperature from 300 K to 400 K. At higher temperature, photovoltaic parameters of a solar cell (electron and hole mobility, carrier concentrations, bandgap) are affected which causes lower efficiency of the cell [21]. Effect of temperature on WS₂ solar cell with different buffer layers is shown in Fig 8.

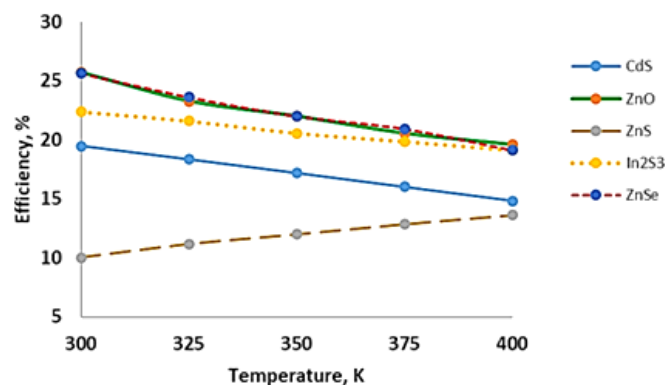


Fig. 8. Effect of temperature on solar cells with different buffer layers

The reverse saturation current increases with the increase of temperature. As V_{oc} is temperature sensitive, the increase in the saturation current decreases the open circuit voltage. This causes electrons to gain more energy at higher temperature and recombined with the holes before they could reach the depletion region and be collected. So, solar cells become unstable at higher temperature [18, 23].

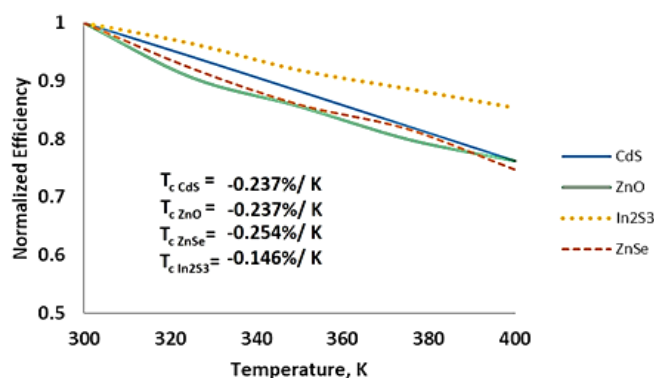


Fig 9. Temperature gradient of WS_2 cell with different buffer layers

To assess the effect of temperature, same structural parameters are used. With CdS as buffer layer, efficiency decreases when temperature is increased with a gradient of $-0.237\%/K$. Other Cd-free buffer layers are also simulated to investigate the effect of temperature on cell performance by varying temperature from 300 K to 400 K. The efficiency of ZnO, In_2S_3 and ZnSe buffer layers based WS_2 solar cells decrease with the increase of temperature at a gradient of $0.237\%/K$, $0.146\%/K$ and $0.254\%/K$, respectively as shown in Fig. 9.

4. Conclusions

In this study, performance of transition-metal dichalcogenide, i.e. WS_2 based solar cells have been investigated from numerical simulation perspective. The main focus was to optimize the thickness of absorber layer as well as to replace CdS buffer layer by other suitable materials. It is revealed that ZnO or ZnSe can substitute widely used CdS buffer layer. The photovoltaic parameters (J_{sc} , η , V_{oc} and FF) have also been investigated in this simulation study.

By analyzing simulation results, it is evident that the solar cell performances are temperature sensitive for all types of buffer layers at various rate of temperature coefficient. Based on optimization, the highest efficiency of 25.71% has been achieved for WS_2 solar cell with 2000 nm thick absorber layer ($J_{sc} = 32.70 \text{ mA/cm}^2$, $V_{oc} = 0.90 \text{ V}$ and FF = 86.5%) and ZnO as buffer layer with 50 nm thickness. However, this optimized WS_2 solar cell with ZnO buffer has temperature degradation coefficient of $0.237\%/K$, which is higher than WS_2 solar cell with ZnS buffer layer.

Acknowledgement

The authors would like to acknowledge and appreciate the contribution of The National University of Malaysia through the research grant with code GUP-2017-031. Appreciations are also extended to CEREM of King Saud University for their contribution through the research grant with code RGP-1438-025.

References

- [1] R. G. Dickinson and L. Pauling, J. Am. Chem. Soc. **45**, 1466 (1923).
- [2] R. G. W. Wyckoff, Crystal Structures (Inter science, New York, 1963).
- [3] H. Tributsch, Ber. Bunsenges. Phys. Chem. **81**, 362 (1977).
- [4] E. Bucher, in: Photo electrochemistry and Photovoltaics of Layered Semiconductors, edited by A. Aruchamy (Kluwer Academic Publishers, Dordrecht, 1992), p. 1.
- [5] H. J. Lewerenz, A. Heller and F. J. Di Salvo, J. Am. Chem. Soc. **102**, 1877 (1980).

- [6] A. Jäger-Waldau, M. C. Lux-Steiner, and E. Bucher, *Solid State Phenom.* **37/38**, 479 (1994).
- [7] A. Matthäus, A. Ennaoui, S. Fiechter, T. Kiesewetter, K. Diesner, I. Sieber, W. Jaegermann, T. Tsirlina, R. Tenne, *J. Electro chem. Soc.* **144**, 1013 (1996).
- [8] Koen De cock, Samira Khelifi, Marc Burgelman, *Thin Solid Films* **2011**, 7481 (2011).
- [9] J.M. Burgelman, *Thin Solid Films* **515**, 6276 (2007).
- [10] M. Burgelman, J. Verschraegen, S. Degrave, P. Nollet, *Modeling thin-film devices, Prog. Photovolt: Res.Appl*, p143 (2004).
- [11] Hossien Movla, *Optimization of the CIGS based thin film solar cells: Numerical simulation and analysis, Optik* **125**, 67 (2014).
- [12] Marc Burgelman, Johan Verschraegen, Stefaan Degrave and Peter Nollet, *Modeling Thin-film PV Devices, Prog. Photovoltaic: Res. Appl.* **12**, 143 (2004).
- [13] J. Marlein, K. Decock, M. Burgelman, *Thin Solid Films* **517**, 2353 (2009).
- [14] P. Nollet, M. Burgelman, S. Degrave, *Thin Solid Films* **361 362**, 293 (2000).
- [15] S. Khelia, J. Verschraegen, M. Burgelman, et al., *Renewable Energy* **33**, 293 (2008).
- [16] Z. Jehl, F. Erfurth, N. Naghavi et al., *Thin Solid Films* **519**, 7212 (2011).
- [17] O. Lundberg, M. Bodeg, J. Malmström, L. Stolt, *Progress in Photovoltaics* **11**, 77 (2003).
- [18] Peijie Lin, Lingyan Lin, Jinling Yu, Shuying Cheng, Peimin Lu, Qiao Zheng, *Journal of Applied Science and Engineering* **17**, 383 (2014)
- [19] Yamamoto, Y. Saito, K. Takahashi, M. Konagai, *Sol. Energy Mat. Sol. Cells* **65**, 125 (2001).
- [20] Puvaneswaran Chelvanathan, Mohammad Istiaque Hossain, Nowshad Amin, *Current Applied Physics* **10**, S387 (2010).
- [21] T. Nakada, M. Mizutani, *Jpn. J. Appl. Phys.* **41**, 165 (2002).
- [22] M. Mostefaouia, H. Mazaria, S. Khelifia, A. Bouraioua, R. Daboua, *Energy Procedia* **74**, 736 (2015).
- [23] F.M.T.Enam et al., *Optik* **139**, 397 (2017).